Short Communication

Corrosion Resistance of Carbon Steel Reinforced Solidia Cement Concrete in corrosive waters: An Electrochemical Impedance Spectroscopy Study

Daoming Shen

School of Civil Engineering and Architecture, Xinxiang University, Xinxiang, 453003, China
E-mail: shendaoming_xx@163.com

Corrosion of embedded steel bars is the main factor that reduces the lifespan of concrete structures, as corrosion products produce tensile stresses which crack the concrete cover. In this research, Corrosion resistance of carbon steel reinforced concrete exposed to corrosive water were investigated using electrochemical impedance spectroscopy technique. The electrolyte solution was prepared using a combination of 3 wt% sodium chloride and 5 wt% sodium sulfate. Samples were exposed to mild water revealed activation signs after a very short period of exposure. It seems that primary activation is a combination of pH 8.8 alkaline and rapid water absorption of the concrete. SEM image of the carbon steel surface in reinforced solidia cement (SC) concrete after 2 months of exposure time indicates a homogeneously distribution of oxide layer on the whole steel surface. The corrosion rate values for SC concrete were very low in aggressive water regime. These results indicate that evolutionary changes of the evaluated SC concrete can act as the effective factors in reducing corrosion.

1. INTRODUCTION

Carbon steel is widely used as alloy for manufacturing and structural uses for construction, metal processing equipment and industries mining [1]. Carbon steel reinforced concrete have better tensile, bending strength and compressive compared to plain concrete structures [2]. However, the structure can be destroyed by the carbon steel corrosion when the passive film is broken on its surface. Corrosion of concrete reinforcement bars is one of the main important phenomena that reduces the life of concrete structures in service, and increases the cost of maintaining the damaged structure [3, 4]. However, these metals are unstable and easily exposed to corrosion. To overcome this issue, numerous

researches are being focused to the development of sustainable and greener concrete structures [5]. The use of stainless steel is one of traditional methods in corrosion resistance [6]. When a material has passivity loss, this can show a pitting corrosion or localized corrosion; it is because of different types of mechanisms: film breakage, pitting and adsorption of contaminants. Fundamentally, carbon steel reinforced concrete shapes a very thin layer which known as the passive layer that is formed because of the high alkalinity of concrete [7]. The layer acts a protective coating and prevents the metal from corrosion. Unfortunately, the layer can be damaged due to chloride ion attack or wither carbonation. Chloride-contaminated aggregates and deicing salts are the main sources of chloride ions formation in concrete [8].

Since concrete is not a homogenous composition, its properties can be widely different with the variation in their proportions in the combination and its components such as the amount and the type of cement, the period and the method of curing and the water/cement ratio [9]. Hence, many researchers motivated to utilize well-controlled synthetic solutions for simulation of concrete environment. The study of the carbon steel corrosion behavior in synthetic solutions which simulates concrete environment started with Hausmann's work [10]. He found the variation of the corrosion potential of the carbon steel specimens after immersing in a saturated calcium hydroxide solution with different chloride concentrations. Later, a significant number of investigations were carried out by other scientists using various electrochemical techniques including potentiodynamic scan [11, 12], open circuit potential (E_{OC}) measurements [13], cyclic polarization [14], potentiostatic scan [15, 16], and electrochemical impedance spectroscopy (EIS) [17-20]. Their main purpose was to discover the critical chloride concentration which causes corrosion of the rebar.

The control of corrosion in ordinary Portland cement concrete is well recognized due to the pH of the pore water in Portland cement (PC)-based concrete is alkaline [21]. Consequently, the reinforcement advances a passive layer that considerably increases the useful life of the structure. Solidia cement (SC) concrete cured through carbonation has a significantly lower pH of the pore water than that of OPC that makes it more difficult to preserve a stable passive layer on the steel. However, a few factors including pH of the pore water affect the corrosion behavior of reinforced concrete structures. The properties of this material, for example high electric resistivity, can be significant factors in reducing corrosion. Furthermore, resistance of rebar corrosion may be different by surface treatment or can be improved using protective coatings. In this research attempts to provide an initial evaluation of the corrosion performance of reinforcing carbon steel in SC-concrete. The evaluation is done to aid potential use of the SC-concrete for construction aims when the structures are exposed to corrosive regimes.

2. MATERIALS AND METHODS

The carbon steel samples as rebar used in this study are prepared from Q235 carbon steel by the following chemical composition: 0.26% Si, 0.46% Mn, 0.17% C, 0.017% S, 0.0047% P and Fe balance. SC was made from the same siliceous and calcareous raw materials as PC (Table 1). All of the pyroprocessing systems used to make PC clinker are valid to the production of SC clinker. The

main difference in pyroprocessing of these two cements is that SC clinker can be produced at about 1200 ℃ temperature. Steel bars were cut and cleaned with silicon carbide paper and then rinsed with water and ethanol.

Table 1. Chemical composition of Portland cement

Oxyde	Mass (%)
Calcium oxide, CaO	63.20
Silicon dioxide, SiO₂	21.35
Aluminium oxide, Al₂O₃	4.33
Ferric oxide, Fe₂O₃	1.95
Sulfur (VI) oxide, SO₃	3.60
LOI	1.60

The SC was made by the combination of 55 wt% Limestone and 45 wt% Shale/Clay/Sand at the maximum furnace temperature of 1200 ℃ by 550 kg CO_2/t and 3.8 Gj energy/t of cement. Mortar was prepared using SC with water/cement ratio of 0.7. Concrete cylinder were formulated with a similar proportion consist of cement, sand and gravel with the ratio of 1:2:4. The dimension of prepared concrete cylinder is as follows, 3.7 cm radius and 11 cm height. A copper wire was utilized for electrical connection. Then the reinforced concrete samples were placed in an environmental chamber at the temperature of 25 ℃ to accelerate the corrosion process of the carbon steel rebar. Figure 1 shows a schematic diagram and detailed dimensions for a reinforced concrete sample. Specimens for corrosion study were partly immersed into corrosive water containing a mixture of 3 wt% sodium chloride and 5 wt% sodium sulfate.
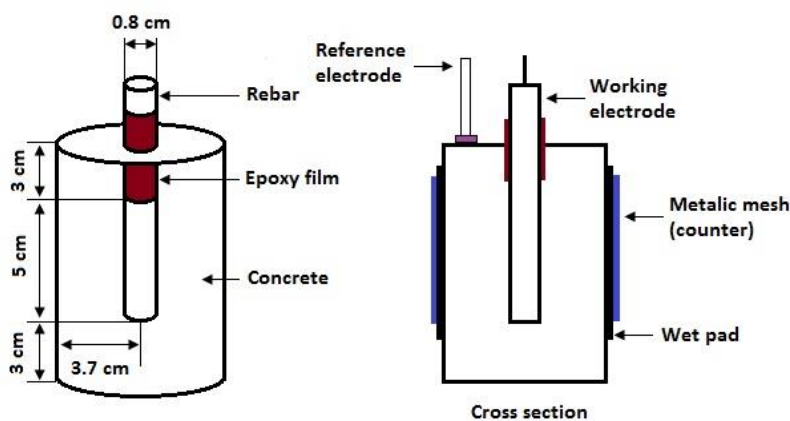
Figure 1. Schematic diagram of the carbon steel reinforced concrete used as a working electrode in electrochemical experiments

EIS measurements were performed using an impedance gain phase analyzer (Solartron-Si1287/Si1260). Three electrode system was employed, including an aforementioned reinforced mortar specimen as a working electrode, saturated calomel electrode as a reference electrode, and titanium mesh to form a counter electrode. EIS spectra were periodically measured in order to analyze the behavior of the different types of concrete during the exposure to aggressive environment. Evaluations were periodically performed after 1, 2, 4 and 6 months of exposure. EIS characterizations were done in the frequency range of 100 kHz to 0.1 mHz at the E_{OC} with AC perturbation ±10 mV. The surface morphology of carbon steel rebars were characterized by scanning electron microscopy (SEM; FEI/Nova NanoSEM 450).

3. RESULTS AND DISCUSSION

In order to describe corrosion activities of the reinforcing carbon steel embedded into a concrete and exposed to an aggressive media, EIS spectra were considered during 6 months' exposure time at the E_{OC}. EIS spectra of two different types of reinforced concrete after 2 months of exposure to a mixture of 3 wt% sodium chloride and 5 wt% sodium sulfate are indicated in Figure 2. At high frequencies, log|Z| vs. Frequency plot shows a slope near to zero reflecting the mortar resistance such as pore solution and bulk material [22]. At mid frequencies, the phase angle near to 80 indicating the capacitive activities at the rebar/concrete interface. At low frequencies, log|Z| vs. frequency and the phase angle plots show a slope decreasing to 0° that can be attributed to the resistance of the charge-transfer processes [23].
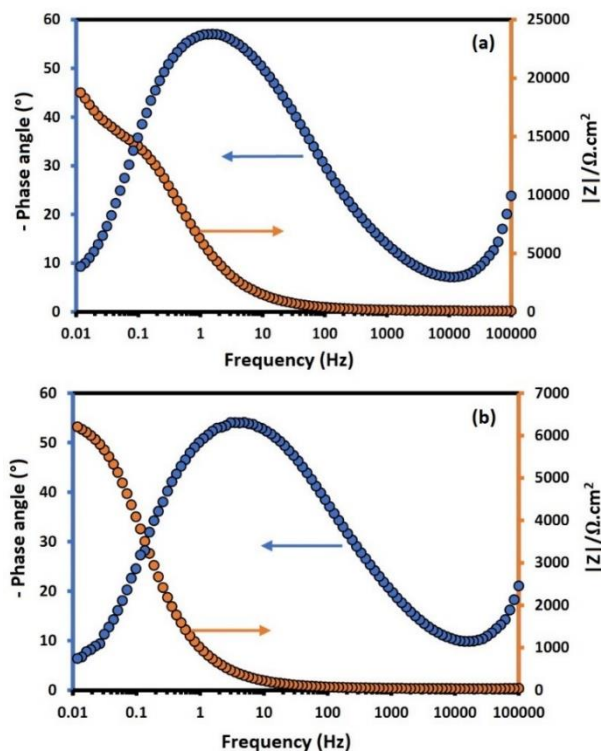
Figure 2. Bode plots of carbon steel reinforced (a) SC (b) PC concretes after 2 months of exposure to a mixture of 3 wt% sodium chloride and 5 wt% sodium sulfate

Repeated characterizations during 2 months of sample exposure to the aggressive water, demonstrated enhancement of impedance module at low and high frequencies for SC-concrete compared by PC-concrete reflecting the improvement of the interfacial and electrolyte resistance and also can be associated to the inhomogeneity of the carbon steel surface induced by the passive film [24]. Fig. 3 reveals the impedance spectra after 1, 2, 4 and 6 months of immersion for reinforced SC and PC concrete samples. Two arcs at low and high frequencies appear in Nyquist plots. These arcs occur due to the two constant times of reactions occurring on the steel surface.
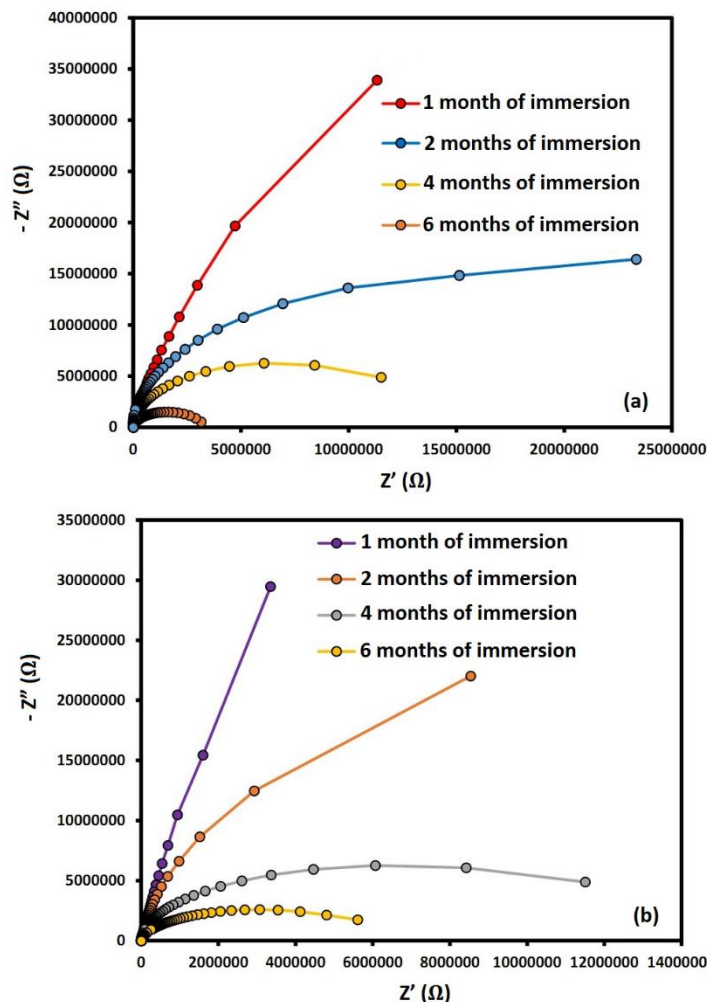
Figure 3. Nyquist plots (a) Reinforced PC concrete and (b) SC concrete after different times of exposure to a mixture of 3 wt. % sodium chloride and 5 wt. % sodium sulfate

The low frequency arcs are related to the interfacial reactions including two processes with an inseparable and similar time constant [25]. The high frequency arcs are associated to the adsorption of hydroxide ions on carbon steel surface [26]. The Nyquist diagrams are showing similar phenomenon in both concretes after one month of exposure time. Furthermore, the polarization resistance and solution resistance during the 6 months of evaluation show high attenuation due to the influence of chloride ion in the structure of concrete. The circuit revealed in Figure 4 was used to model the parameters found in

the analyzed system. During the passivity period, the second time constant parameters were becoming visible at the low frequencies (R_2, CPE2) was associated to the charge transfer resistance and non-ideal interfacial capacitance of the steel surface that revealed the corrosion resistance of the steel surface controlled through the properties of passive film [27]. The first time constant parameters were becoming visible at the intermediate frequencies (R_1, CPE1) which appeared to be correlated with a redox transformation of the corrosion products that had occurred on the oxide film surface [28]. The presence of the two time constants at the existing impedance spectra was not always clear, but in order to attain the results with satisfying accuracy, the data related to the electrical circuit that were equivalent to the parallel distribution was necessary. The values of CPE1 and R_1 calculated at the intermediate frequencies indicated a significant oscillation because of the limitations in spectra analysis derived from overlapment of the peaks. The values of R_1 were similar for all tested steels and were considerably lower compared to the R_2 for all the specimens.
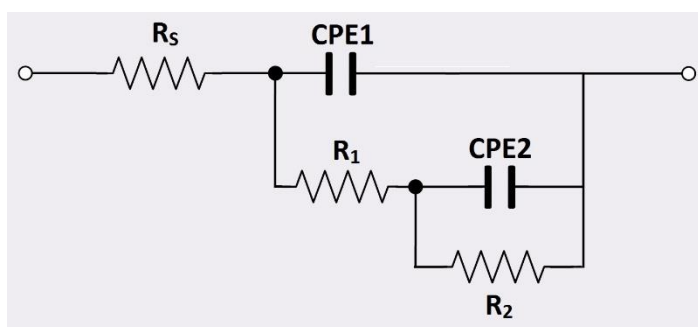
Figure 4. Equivalent electrical circuit model reproducing the impedance data
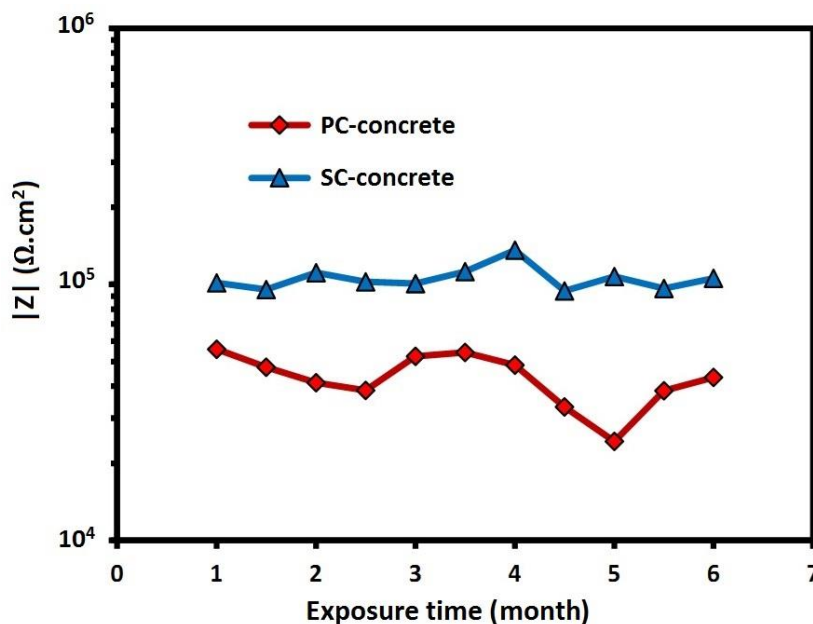
Figure 5. Resistance dependence on exposure time for PC and SC concrete at low frequency

This method was employed to electrochemically explain the influence of corrosive water in the breakdown of the steel passivity which was the best fit due to the first resistance was related to preventing the entry of solution ions into a concrete. The first resistance value was small, since the amount of ions at the initial levels was minimal, thus easily influenced the concrete. The decrease of polarization resistance value indicated an increase in the corrosion rate. The constant phase element of the interface which was parallel to the polarization resistance was showing a drop. The element had made a greater influence of ions on the steel surface which had led to more deterioration on rebar surface. Furthermore, a comparison of the Nyquist plots between reinforced SC and PC concretes at the same exposure time shows that SC concrete has a higher corrosion resistance than PC concrete, indicating a good alternative material to traditional PC concrete.

As shown in figure 5, SC concrete indicates higher impedance values (10^5 $\Omega.cm^2$) in comparison of reinforced PC concrete (4×10^4 $\Omega.cm^2$). Results obtained in solutions simulating the reinforced concrete from literature, contaminated with chloride ions reveal that carbon steel reinforced SC concrete shows higher performance reasonably to the PC concrete [4, 29], that is in accordance with the attained results.
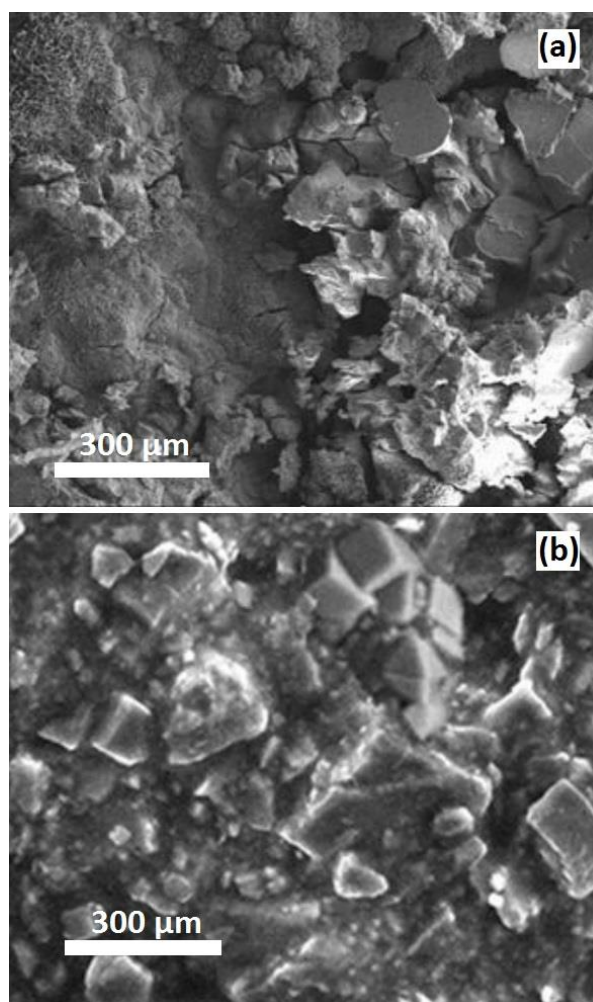
Figure 6. SEM images of the surface of carbon steel reinforced (a) SC and (b) PC concretes after 2 months of exposure to a mixture of 3 wt. % sodium chloride and 5 wt. % sodium sulfate

Figure 6 shows the SEM images of the microstructure of the carbon steel embedded in the PC and SC concretes after 2 months of exposure times. As shown in Figure 6a, the corrosion products are formed on the steel surface of SC concrete, it is clearly seen that an oxide layer covers the whole surface. Furthermore, the corrosion products are homogeneously distributed due to the nonexistence of cracks in the surface.

Figure 6b indicates the corrosion products were also generated on the carbon steel surface of the PC concrete after 2 months of exposure in the corrosive waters. It was found that the same corrosion products formed on the surface of carbon steel with porous aspect effected by corrosion phenomenon in the chloride ion influences which produced this type of degradation.

4. CONCLUSION

Reinforced concretes manufactured by a developing type of Solidia Cement mortar and carbon steel rebar are considered using an electrochemical impedance technique. The corrosion behavior of rebar was assessed for about 6 months of exposure times in the corrosive water including a combination of 3 wt. % sodium chloride and 5 wt. % sodium sulfate. SEM images of the carbon steel surface embedded in the SC concrete indicate that an oxide layer covered the whole steel surface which were homogeneously distributed due to the nonexistence of cracks in the surface. The SC concrete evaluated revealed higher values of corrosion resistivity than traditional PC concrete in the same conditions. The higher resistivity can be a significant factor in limitation of corrosion rate.

References

1.   I. Duarte, L. Krstulović-Opara and M. Vesenjak, *Compos. Struct.*, 152 (2016) 432.
2.   T. Ji, F. Ma, D. Liu, X. Zhang, X. Zhang and Q. Luo, *Int. J. Electrochem. Sci.*, 13 (2018) 5440.
3.   C.G. Berrocal, K. Lundgren and I. Löfgren, *Cem. Concr. Compos.*, 80 (2016) 69.
4.   J. Rivera-Corral, G. Fajardo, G. Arliguie, R. Orozco-Cruz, F. Deby and P. Valdez, *Constr. Build. Mater.*, 147 (2017) 815.
5.   B. Suhendro, *Procedia Eng.*, 95 (2014) 305.
6.   A. Fahim, A.E. Dean, M.D. Thomas and E.G. Moffatt, *Mater. Corros.*, 70 (2018) 328.
7.   J. Williamson and O.B. Isgor, *Corros. Sci.*, 106 (2016) 82.
8.   J. Wu, H. Li, Z. Wang and J. Liu, *Constr. Build. Mater.*, 112 (2016) 733.
9.   S.-H. Kang, S.-G. Hong and J. Moon, *Cem. Concr. Compos.*, 89 (2018) 130.
10.   D. Hausmann, *Mater. Protect.*, 6 (1967) 19.
11.   C. Frazão, J. Barros, A. Camões, A.C. Alves and L. Rocha, *Cem. Concr. Compos.*, 79 (2016) 112.
12.   U. Angst, M. Büchler, J. Schlumpf and B. Marazzani, *Mater. Struct.*, 49 (2016) 2807.
13.   G. Liu, Y. Zhang, Z. Ni and R. Huang, *Constr. Build. Mater.*, 115 (2016) 1.
14.   V. Maruthapandian, S. Muralidharan and V. Saraswathy, *Constr. Build. Mater.*, 107 (2016) 28.
15.   H.W. Ashadi, B.A. Aprilando and S. Astutiningsih, *Int. J. Technol.*, 6 (2015) 227.
16.   R. Blair, B. Pesic, J. Kline, I. Ehrsam and K. Raja, *Acta Metall Sin-EngL.*, 30 (2017) 376.
17.   S.P. Arredondo-Rea, R. Corral-Higuera, J. Gómez-Soberón, D.C. Gámez-García, J. Bernal-Camacho, C. Rosas-Casarez and M. Ungsson-Nieblas, *Appl. Sci.*, 9 (2019) 617.
18.   W. Miao, Z. Gao and W. Hu, *Int. J. Electrochem. Sci.*, 13 (2018) 771.
19.   G. Xie and L. Wei, *Int. J. Electrochem. Sci.*, 13 (2018) 5311.

20.   F. Vázquez-Rodríguez, A. Arato, D.I. Martínez-Delgado, A. Guzmán, N. Elizondo-Villarreal, R. Puente-Ornelas and E. Rodríguez, *Int. J. Electrochem. Sci.*, 13 (2018) 6027.
21.   J.M. Paris, J.G. Roessler, C.C. Ferraro, H.D. DeFord and T.G. Townsend, *J. Clean. Prod.*, 121 (2016) 1.
22.   M. Criado and J.L. Provis, *Front Mater.*, 5 (2018) 1.
23.   Z. Salarvand, M. Amirnasr, M. Talebian, K. Raeissi and S. Meghdadi, *Corros. Sci.*, 114 (2017) 133.
24.   A. Sagüés, S. Kranc and E. Moreno, *Corros. Sci.*, 37 (1995) 1097.
25.   M. Khan, A. Amari, A. Mustafa, H. Shoukry, I.H. Ali, S.A. Umoren and A.M. Kumar, *Int. J. Electrochem. Sci.*, 13 (2018) 7385.
26.   N. Nam, P. Ha, H. Anh, N. Hoai and P. Hien, *J. Saudi Chem. Soc.*, 23 (2019) 30.
27.   H. Luo, C. Dong, X. Li and K. Xiao, *Electrochim. Acta*, 64 (2012) 211.
28.   A. Bautista, A. González-Centeno, G. Blanco and S. Guzmán, *Mater. Charact.*, 59 (2008) 32.
29.   W. Nguyen, J.F. Duncan, T.M. Devine and C.P. Ostertag, *Electrochim. Acta*, 271 (2018) 319.